Int. J. Electrochem. Sci., 8 **(2013)** 1722 - 1734

International Journal of
ELECTROCHEMICAL
SCIENCE
www.electrochemsci.org

Development of Electroless Ni-P-Al_2O_3 and Ni-P-TiO_2 Composite Coatings from Alkaline Hypophosphite Gluconate Baths and their Properties

S.A. Abdel. Gawad[1],[*] *A.M. Baraka*[1] , *M.S. Morsi*[1] *and M.S. Ali Eltoum*[2]

[1]Chemistry Department, Faculty of Science, Cairo University, Cairo, Egypt
[2]Scientific Laboratories Department, Faculty of Science, Sudan University, Khartoum, Sudan
[*]E-mail: dr_m_saber@live.com

Received: 27 September 2012/ *Accepted:* 25 December 2012 / *Published:* 1 February 2013

The performance of electroless deposited Ni-P-alumina and Ni-P-titania, composite coatings from alkaline hypophosphite gluconate baths, on copper substrate was studied. The effect of both TiO_2 and Al_2O_3 (g/L) on the deposition rate of Ni-P-TiO_2 and Ni-P-Al_2O_3 alloys respectively were investigated. The amount of particles incorporated in the coatings increased with increasing particle concentration in the bath. However, the particle size greatly affected the amount incorporated. The addition of these particles changed the microstructure of the Ni-matrix, and enhanced the hardness and corrosion resistance. Also, the coating brightness, coherence and uniform surface distribution were improved. The changes in the hardness and structure of deposits were studied by X-ray diffraction, scanning electron microscopy and energy-dispersive x-ray spectroscopy methods.

Keywords: Ni-P-Al_2O_3 composite coatings, Ni-P-TiO_2 composite coatings, gluconate baths**,** electroless Ni coatings, Ni-alloys, matrix composite, alkaline hypophosphite baths, corrosion resistance.

1. INTRODUCTION

Nickel–phosphorous (Ni–P) coatings are widely used in many industrial applications due to their outstanding mechanical and chemical properties, such as high hardness and good corrosion / wear-resistance [1 – 3]. Ni–P coatings can be fabricated by various techniques including electro-plating [4] and electroless deposition [5, 6]. Metals can be protected from abrasion, by coating them with metallic composite containing particles of Al_2O_3 or TiO_2. These hard materials are too brittle and offer little or no adhesion potential to be used alone as a coating material. Therefore, a metal matrix is

used to hold Al_2O_3 or TiO_2 particles together and facilitate good adhesion to the metal surface being coated. These composites have a considerably higher yield strength and hardness than that the pure metal exhibits [7]. Composite coatings can also reduce the corrosion of low alloys [8]. The high temperature oxidation resistance of Ni-P alloys has been significantly increased by the addition of Al_2O_3, matching a decrease in the rate of oxidation with increasing volume percent of Al_2O_3 in the composite [9]. This suggests that electroless Ni-P-Al_2O_3 composite coatings should offer good wear and corrosion properties at high temperatures [10].

The structure of as-deposited electroless Ni-P is amorphous with high phosphorus content. However, this amorphous structure is metastable and undergoes a crystalline transition with increasing temperature. After adequate heat treatment, the coating becomes crystalline and its hardness and wear resistance are greatly improved [11] Embedding particles in electroless deposited metals is a convenient method of preparing composite coatings, and the particles increase the mechanical and physical properties of the coating [12]. The activation energy of crystallization is lowered due to the presence of co-deposited particles in composite coating [13]. The effect of particle size has been studied [14]. Greater particle incorporation and uniform distribution was found in composite coatings obtained with 1.0 μm than with 50 nm or 0.3 μm particle sizes. Using a complexing agent such as citrate [15], propylene glycol and urea [16] in electroless Ni-P is found to induce stability during plating. A survey of the literature shows that gluconate electrolytes have been used to electroplate metals such as nickel [17], copper [18], tin [19] and zinc [20]. The investigation of the influence of gluconate on the electroless deposition of Ni–Cu–P alloys is the only literature found for the use of gluconate in electroless nickel plating [21].

The objective of the present study is to obtain Ni-P-Al_2O_3 and Ni-P-TiO_2 composites from alkaline gluconate baths, studying the dependence of coating characteristics on several electroless plating variables. Our work also characterizes the coatings by using different analytical techniques such as SEM, EDX and XRD and examines the coating hardness and corrosion resistance.

2. EXPERIMENTAL

2.1 Pretreatment and activation of copper substrate

Copper sheets of dimensions 2×2 cm were used as substrates. They were mechanically polished with different grade emery papers and then immersed in a pickling solution (300 mL H_2SO_4 + 100 mL HNO_3 + 5 mL HCl + 595 mL doubly distilled water) for 1 min, washed with distilled water and rinsed with acetone. After treatment, the copper substrate was immersed for 20 sec in a dilute acidic solution of $PdCl_2$ (0.1 g/L $PdCl_2$ + 0.2 ml/L 36% HCl), followed by thorough rinsing. Finally, the substrates were dried and weighed [22].

2.2 Electroless nickel deposition

There are three bath compositions were suggested in this study, for the electroless deposition of Ni-P, Ni-P-Al_2O_3 and Ni-P-TiO_2 alloys, where, the bath compositions are respectively:

Bath (A); 25 g/L Nickel sulfate, 15 g/L Sodium hypophosphite, 15 g/L Sodium gluconate, 15 g/L Ammonium sulfate, 0.3 g/L Succinic acid, 0.1 g/L Sodium dodecyl sulfate and 2 mg/L Lead acetate.

Bath (B); Bath (A) in addition to10-90 g/L Alumina (70 nm)

Bath (C); Bath (A) in addition to 1-6 g/L Titania (50 nm)

They were freshly prepared from analytical grade chemicals and doubly distilled water. The electrochemical cell was connected by immersing the copper substrate in 250 mL of the electroless solution for 60 min. The pH was measured using a pH Meter (Model CP 5943-45USA), and adjusted with NH_4OH solution. The temperature was controlled by using a thermostatically-controlled bath. The deposited weight was evaluated from the change in weights of the substrates before and after the electroless process.

2.3 Determination of the coatings composition

The composition of the coatings was evaluated using the following procedure:
1- The coating layer was stripped using 10% H_2SO_4 solution. The specimen was made the anode in an electroplating cell in which the coating layer is dissolved in the solution, which is then diluted to 250 mL with doubly-distilled water.

2-The analysis was done using atomic absorption spectrophotometry (Perkin-Elmer 3100, Germany).

3-The solution obtained in (1) was further diluted by dissolving 5 mL in doubly-distilled water to 250 mL.

4-Nickel standard solutions for the elements to be detected were prepared (1.0 g Ni metal in (1+1) HNO_3. Diluted to 1.0 L with 1.0 vol% HNO_3) , Ni, air-acetylene flame gases and standard wavelength of 232 nm.

5- The phosphorus weight was calculated by subtracting the nickel and alumina or titania weights from the total deposited weight. (The results were confirmed for some samples with EDX analysis.)

6- The deposited mass of nickel *"w"* on the unit surface during the plating time represents the deposition rate "R" [23]: hence, $dR = dw / dt$

2.4 Surface investigation:

The surface morphology of the as-deposited Ni-P-Al_2O_3 and Ni-P-TiO_2 composites on copper was studied using scanning electron microscopy (JEOL-5410 attached to an EDX unit). The surface phases and phase changes of the different coated substrates was studied with an x-ray diffractometer (Broker AXS-D8 x-ray diffractometer, ADVANCE, Germany), with a copper target (λ_{Cu} = 1.54060Å) and a nickel filter.

The Vickers micro hardness of the deposits and the specimen material was measured under a 50-gram load, using a Shimdzu hardness tester.

2.5 Electrochemical processing:

The electrochemical experiments were performed using a Volta Lab 40 (Model PGZ301), with the aid of commercial software (Volta Master 4, V 7.08), which calculates and displays the corrosion rate in μm/yr. The reference and auxiliary electrodes were a saturated calomel electrode (SCE) and a platinized platinum black electrode, respectively. The electrolyte used was a 3.5% NaCl solution.

3. RESULTS AND DISCUSSION

3.1 Optimization of Ni-P alloy electroless deposition parameters:

When Bath (A) operated at working conditions pH 9, temperature 90°C and duration time 60 min, increasing the hypophosphite concentration in the plating bath (from 5 to 30 g/L) increases not only the deposition rate "DR" ($mg/cm^2.hr$), but also the phosphorus content of the deposits as indicating from Fig (1). The deposition rate not changed after the addition of 30g/L sodium hypophosphite, This is due to the fact that even though the available electrons for metal ion reduction increases with increase in concentration of hypophosphite, the rate at which the availability of the metal ion is limited by the amount of complexing agent present in the bath.

Deposition rate "DR" ($mg/cm^2.hr$), at the same working conditions was increased by increasing the nickel ions concentration (from 5to 35g/L), and sodium gluconate concentration (from 10 to 50 g/L), as shown in Fig (2), while keeping all the other bath constituents constant. Sharp decrease observed after the addition of 50g/L of the sodium gluconate, which attributed to the inhibiting effect of the gluconate salt.

When the bath composition kept constant, while, changing the bath pH, it was found that the deposition rate increased as the pH increases up to pH9, then decreased sharply after that. Also, the P% increased with the solution pH up to pH 9 and after that the P% decreased as results of precipitation of phosphate ions, nickel salts and nickel hydroxide, Fig (3).

Deposition rate of electroless nickel is increased as Increasing both of temperature and time, and this was shown in Fig (4), as the plating time increasing throughout 60 minute plating, and this due to autocatalytic nature of the electroless plating process. However, the increase in thickness is not the same throughout the entire duration of plating.

EDX pattern of Ni_{96}-P_4 and Ni_{82}-P_{18} alloy respectively, and XRD patterns of the Ni-P deposits were shown in Fig (5 & 6), where only one broad peak with a weak intensity appeared at about $2\theta = 45°$ implying that the deposits were amorphous. This result is in agreement with result obtained by Gao Rongjie et.al [24].the crystal size was 16.84nm.

3.2 Micro structure and Microhardness of Ni-p alloy:

The Ni-P as plated deposits has amorphous structure as indicated from SEM results, Fig (7). The hardness of Ni-P alloy decreased as the phosphorus content in the alloy increased. The heat of the

deposits is also increased the hardness, the observed hardness fore Ni_{96}-P_4 coating without heat treatment was 490HV_{50}.

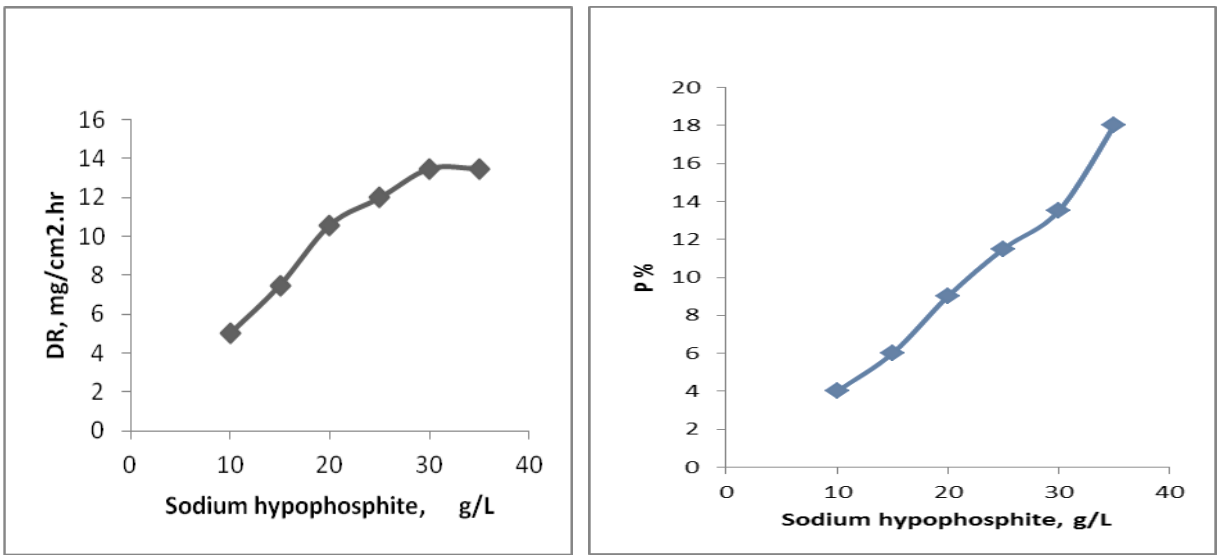

Figure 1. Effect of Sodium hypophosphite g/L, on DR and phosphorous % from operated at . . working conditions pH 9, 90°C and duration time 60 min.

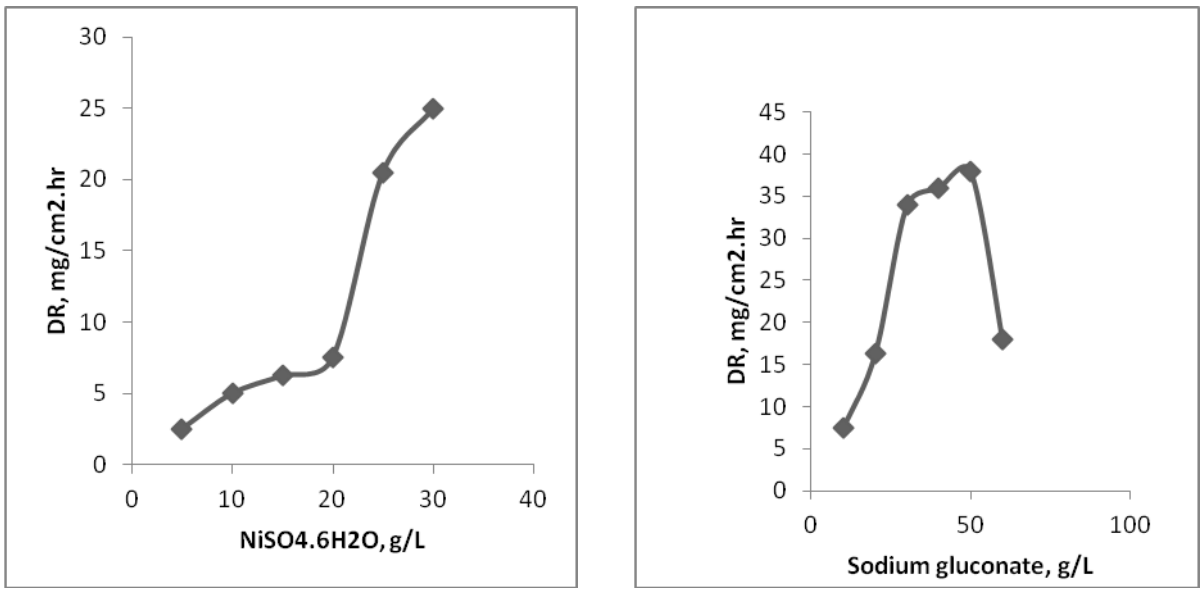

Figure 2. Effect of $NiSO_4.6H_2O$ (g/L) and Sodium gluconate (g/L) on DR from bath "A" operated at working conditions pH 9, 90°C and duration time 60 min.

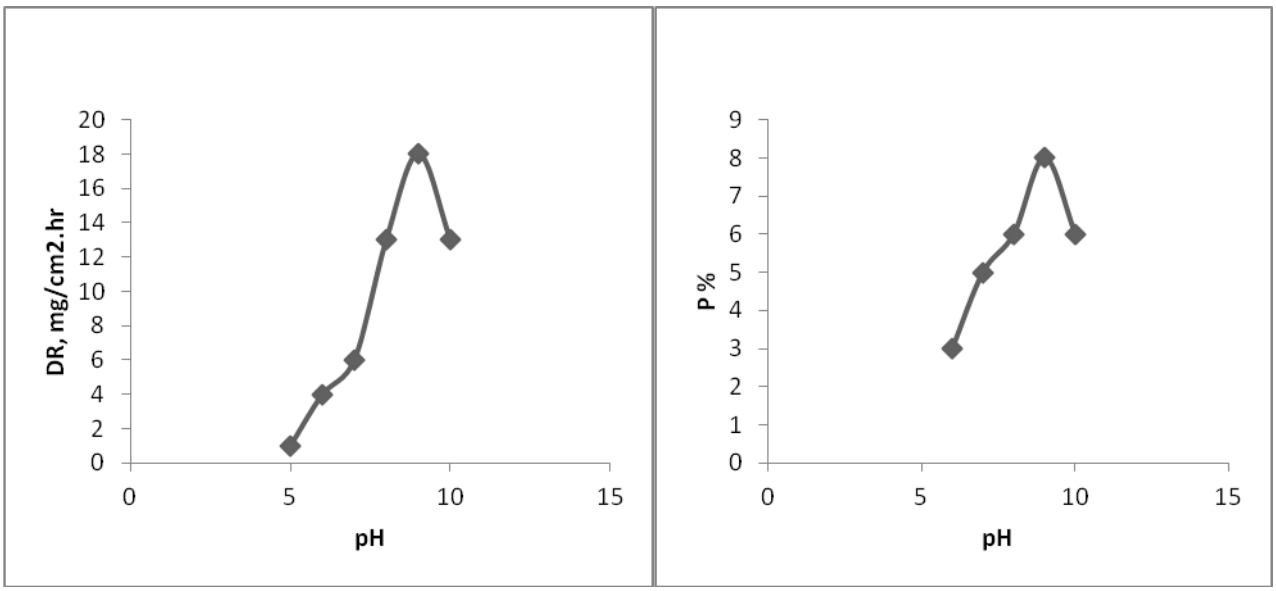

Figure 3. Effect of pH, on DR and phosphorous % from bath "A" operat

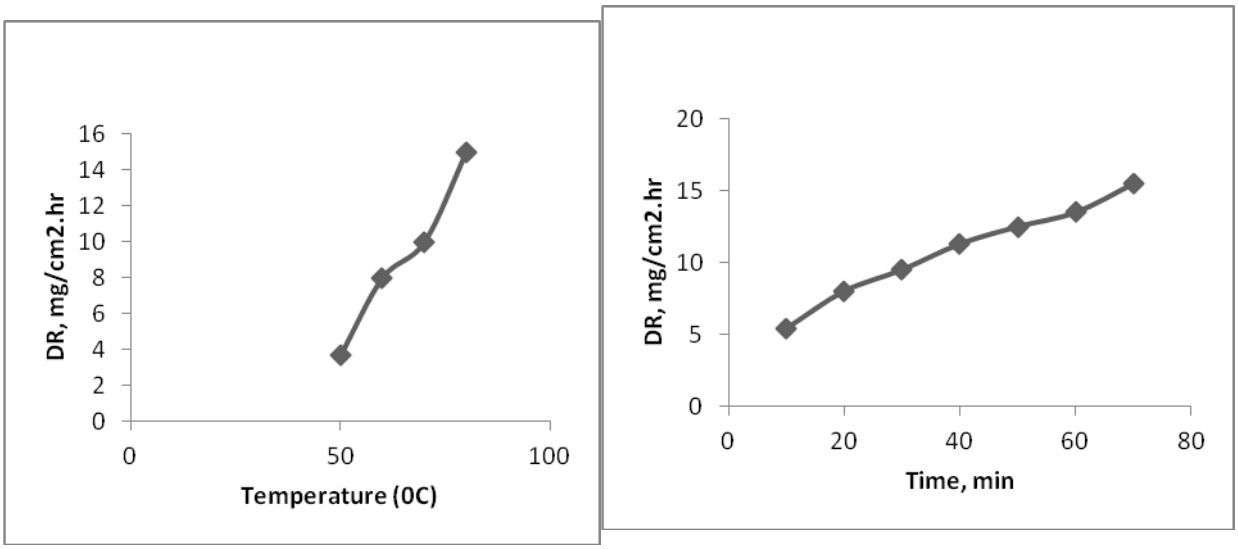

Figure 4. Effect of temperature ($^{\circ}$C) and time (min) on DR from bath **"A"**

3.3 Effect of alumina and titania on Ni-P electroless deposition

The optimum conditions of Ni-P plating were operated for baths "B" and "C". It was found that the deposition rate increased with increasing alumina concentration up to 70 g/L for bath "B", and then decreased as the alumina content in the bath increased further as shown in Fig (8,a). The alumina content in the deposit also increased in the same manner as shown in Fig (8, b). This limiting content corresponds to steady state equilibrium, whereby the number of co-deposited particles equals the number approaching the substrate surface. Beyond the optimum concentration, suspended particles appeared to agglomerate in the bath. Accordingly, the decreasing trend of incorporation of alumina particles was observed.

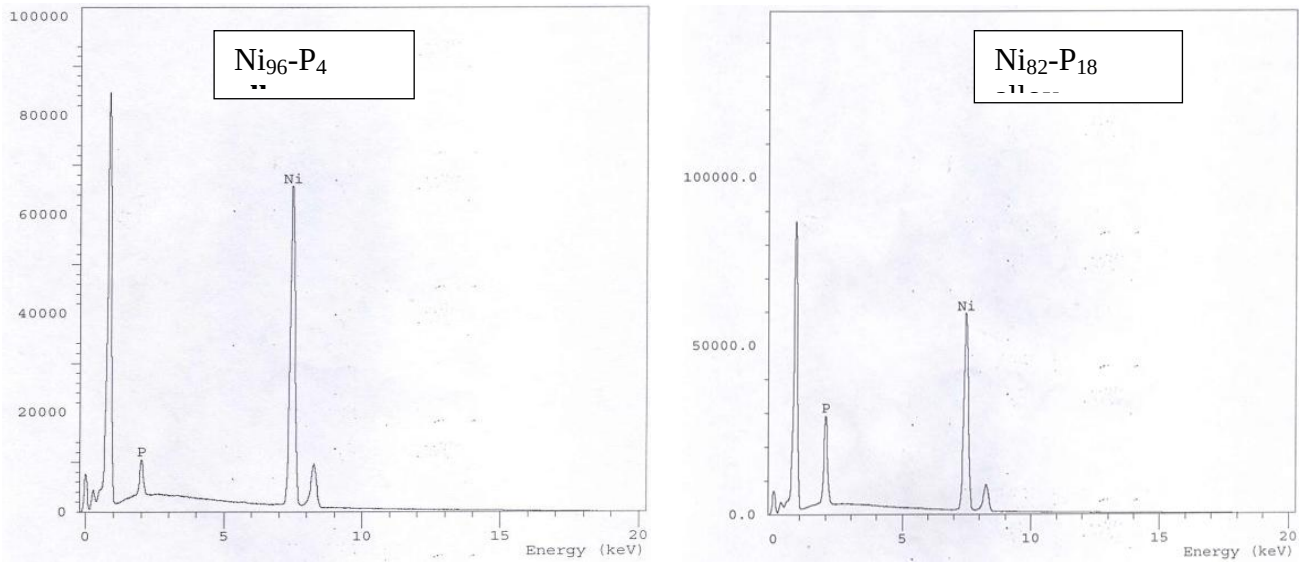

Figure 5. .EDX chart of Ni_{96}-P_4 and Ni_{82}-P_{18} alloys d from bath "A "operated at working conditions pH 9, 90°C and duration time 60 min.

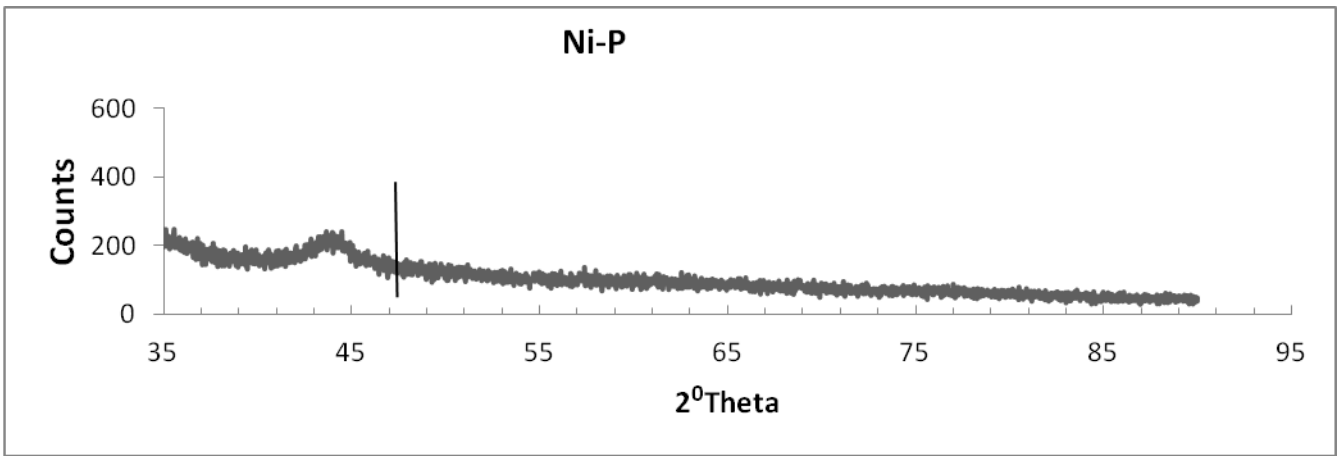

Figure 6. XRD chart of Ni_{82}-P_{18} alloy from bath "A "operated at working conditions pH . 9, 90°C and duration time 60 min.

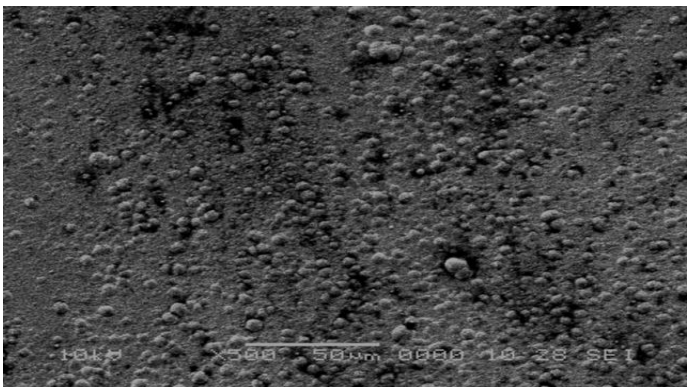

Figure 7. SEM of Ni_{82}-P_{18} alloy from bath "A "operated at working conditions pH9, 90°C and duration time 60 min.

The same behavior was observed through the change of TiO_2 content(g/L) in bath "C", where, the deposition rate increased with increasing titania content in the bath as shown in Fig (9,a). Fig (9, b) shows the TiO_2 content in the deposit increased with increasing TiO_2 nanoparticle concentration in the plating bath. The nickel films from the alkaline bath contained significantly higher amounts of particles. There seems to be a tendency that negatively-charged oxide particles are preferentially codeposited in cathodic processes, at least in solutions containing divalent cations. To explain this counter-intuitive behavior, an electrostatic model has been proposed [25, 26] that takes into account the charge distribution on the particle and the electrode surface. In the alkaline electrolyte the TiO_2 nanoparticles are negatively charged, whereas in the acidic one they bear a positive charge. Under the conditions of the nickel electroplating process, the electrode bears negative excess charges [27]. According to the model, negatively charged particles are preferentially attracted by the positive excess charges in the electrolytic part of the electrical double layer of the electrode. When the particle has come close to the electrode, the shell of adsorbed ions on the particle is stripped off within the electrical double layer of the electrode. Finally the particle becomes incorporated into the growing metal layer.

The major challenges for the codeposition of ceramic particles seem to be the occlusion of a sufficient number of non-agglomerated particles combined with a good dispersion of the particles in the metal matrix. In general, it has been observed that the amount of embedded ceramic particles increases with increasing concentration of suspended particles in the electrolyte [28]. Additionally, the reduction of particle size increases the agglomeration tendency of the particles, due to their enhanced surface energy, while decreasing their codeposition content in the metal matrices and the mean grain size of the matrix crystallites [29]. Moreover, research has pointed out that the physico-chemical properties of the ceramic particles are crucial to the understanding of the codeposition mechanism of each type of particle [30].

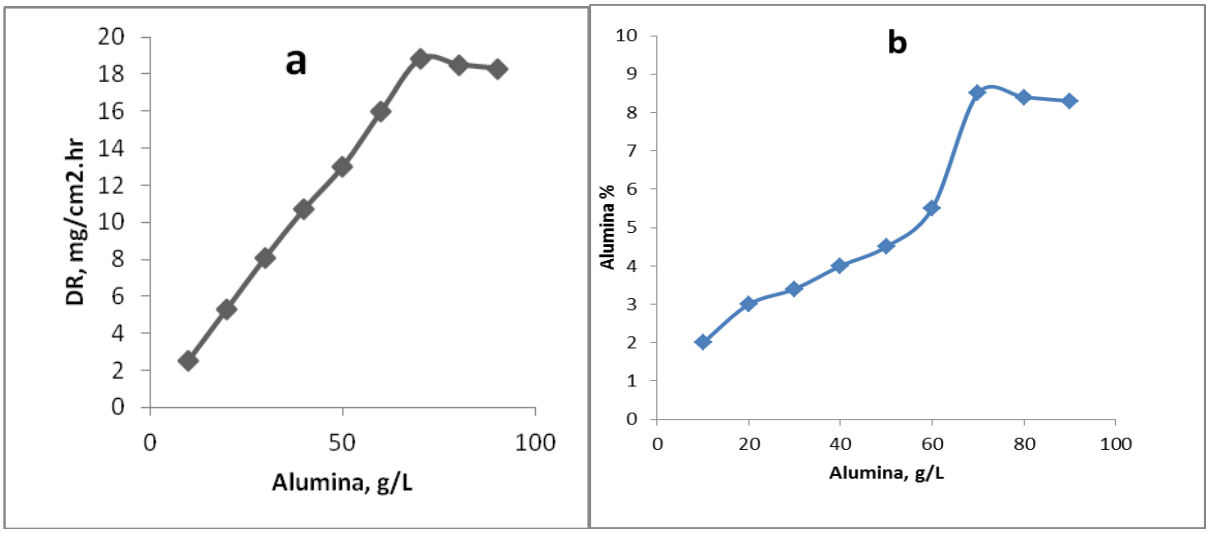

Figure 8. Effect of alumina concentration on the deposition rate and alumina content in the Ni-P-Al_2O_3 alloy from bath "B".

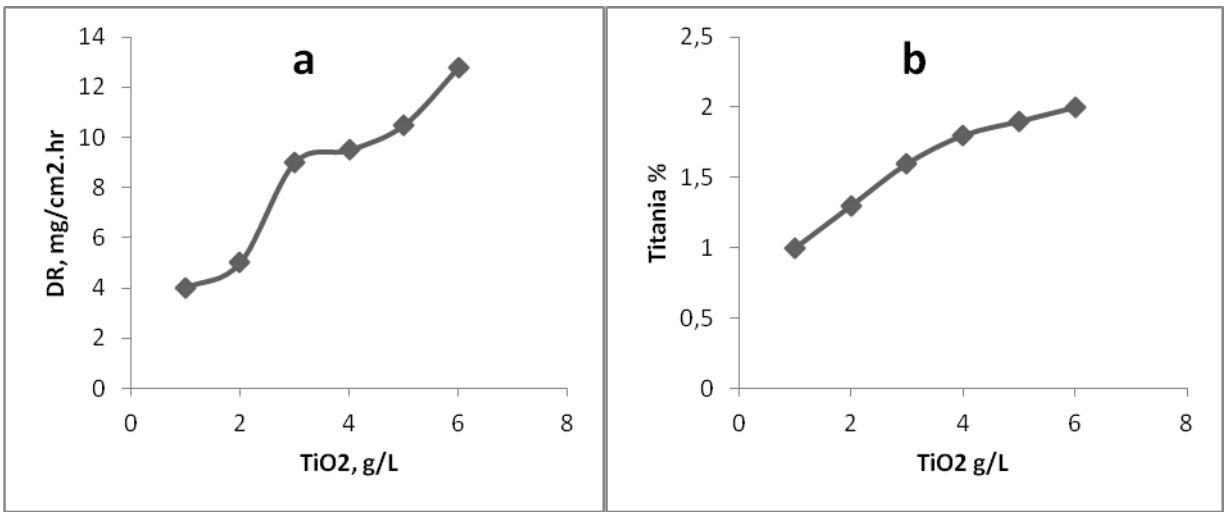

Figure 9. Effect of TiO_2 concentration on the deposition rate and alumina content in the Ni-P-Al_2O_3 alloy from bath "B".

EDX chart of 90% Ni-6% P-4% Al_2O_3 alloy with 40 g/L alumina in the bath "B" and that of Ni90%-P8%-$TiO_2$2% alloy with 6.0 g/L TiO_2 load in the bath "C" were shown in Fig(10), The reason that the titania incorporation from the bath (40 g/L ⇒ 4%; 10:1) is higher than alumina (6 g/L ⇒ 2%; 3:1) can be explained from the difference in in the size is a very important factor.

The addition of alumina nanoparticles to the bath obviously affects the crystal orientation of the coatings as indicated from the x-ray diffraction spectra Fig(11). The peak width for the alumina Fig (11, A) was narrower than the peak obtained for the Ni-P alloy Fig (11, C), indicating a change from the amorphous structure. The appearance of the different peaks of Ni-P and Al_2O_3 without heat treatment is not fully understood. The grain size was 34.5 nm for the alumina sample versus 16.84 nm in the case of the Ni-P alloy. In the XRD pattern of the Ni-P-TiO_2 alloy Fig (11, B), the reflections corresponding to the (111), (200) and (220) planes of a face centered cubic (fcc) phase of nickel could be observed. The broad peak is evidence of an amorphous structure. The crystal size was 24 nm.

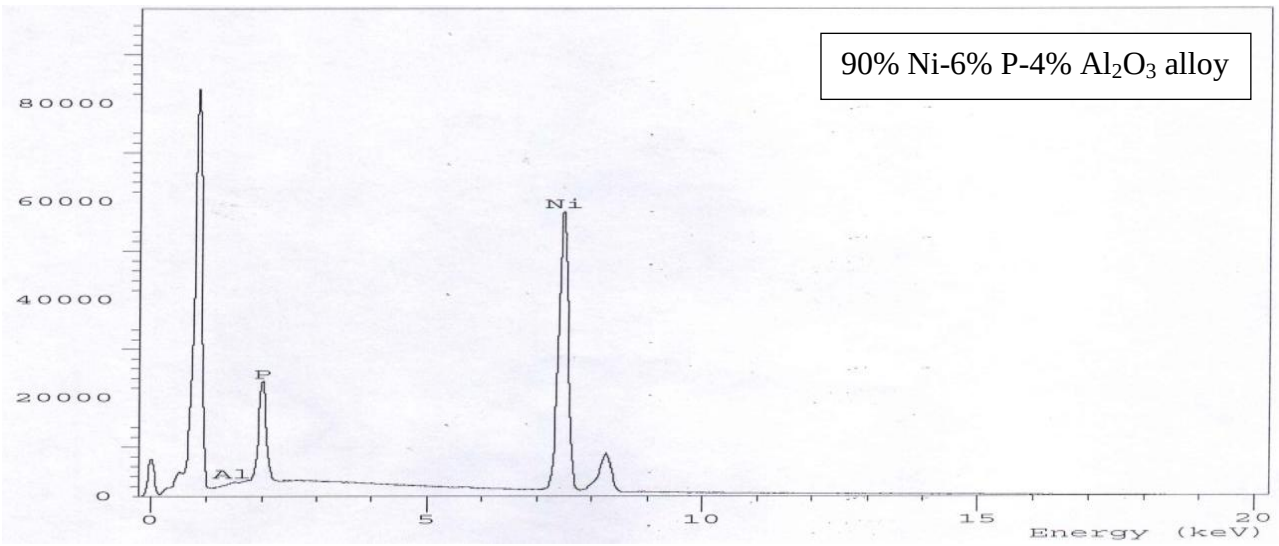

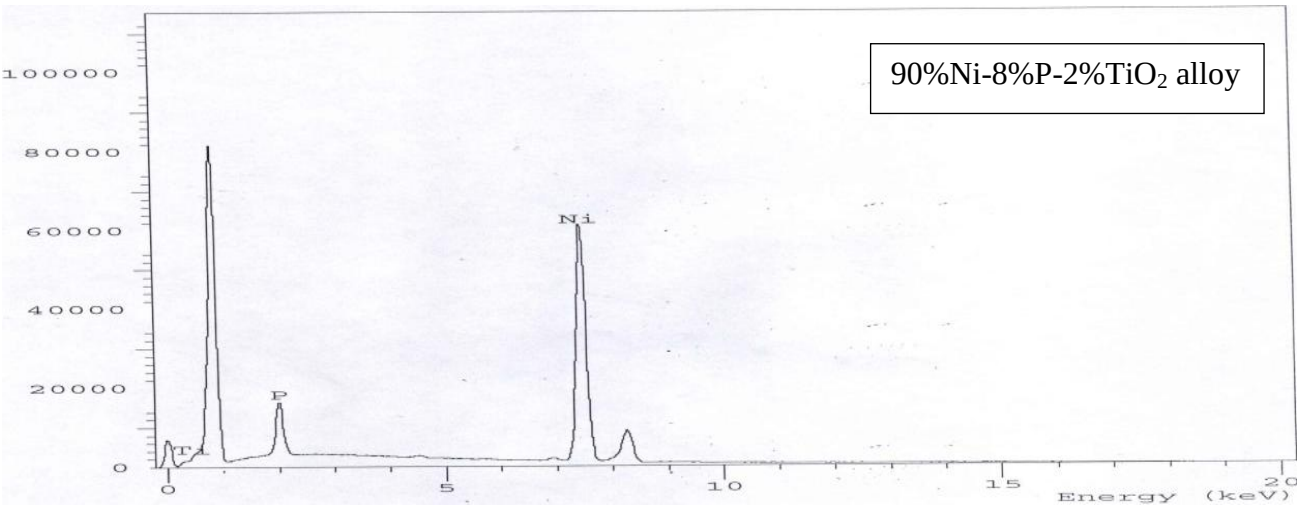

Figure 10. EDX chart of 90% Ni-6% P-4% Al_2O_3 and 90% Ni-8% P-2% TiO_2 alloys

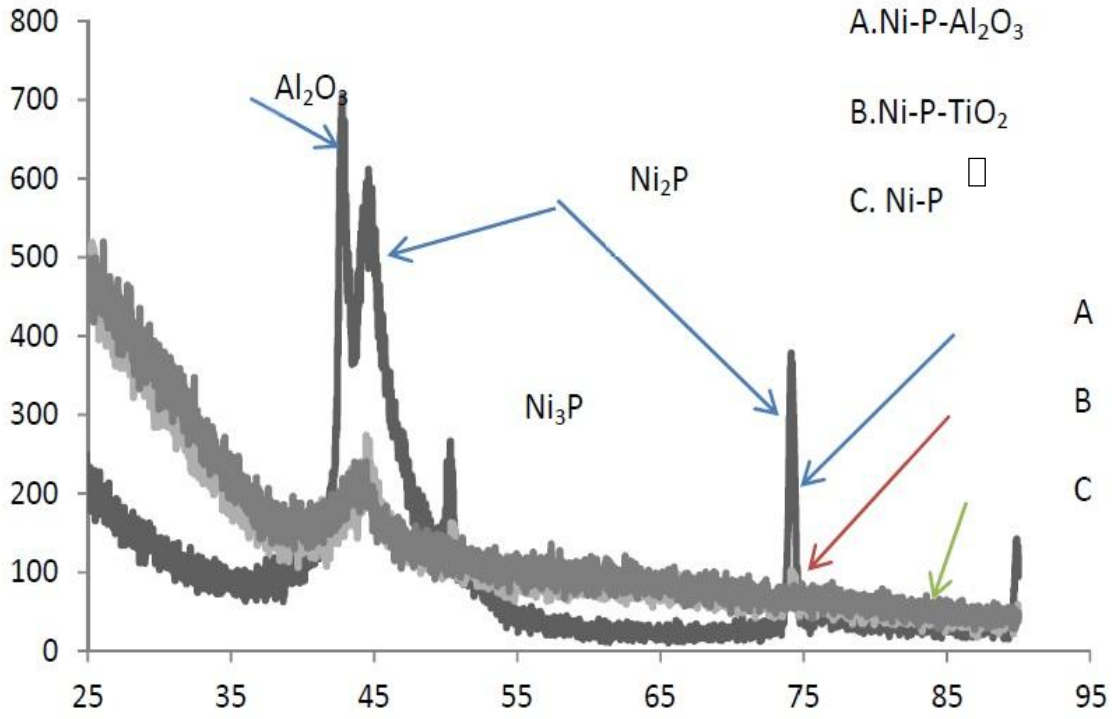

Figure 11. X-ray diffraction spectra of (a) 90% Ni-6% P-4% Al_2O_3, (b) 90% Ni-8% P-2% TiO_2 and (c) 82% Ni-18% P.

3.4 Surface morphology

It is clear from Fig. 12 that the amorphous structure of the Ni-P alloy (Fig.12,a) was changed to a uniform distribution of embedded particles on the coating surface in the case of Ni-P-Al_2O_3 (Fig. 12,b) and Ni-P-TiO_2 (Fig. 12,c). It has been shown that the structure and morphology of the nickel

matrix composites depend on the physicochemical properties, and the particle size and concentration in the bath. A parallel study by Zhou, *et al* [31], showed the same results.

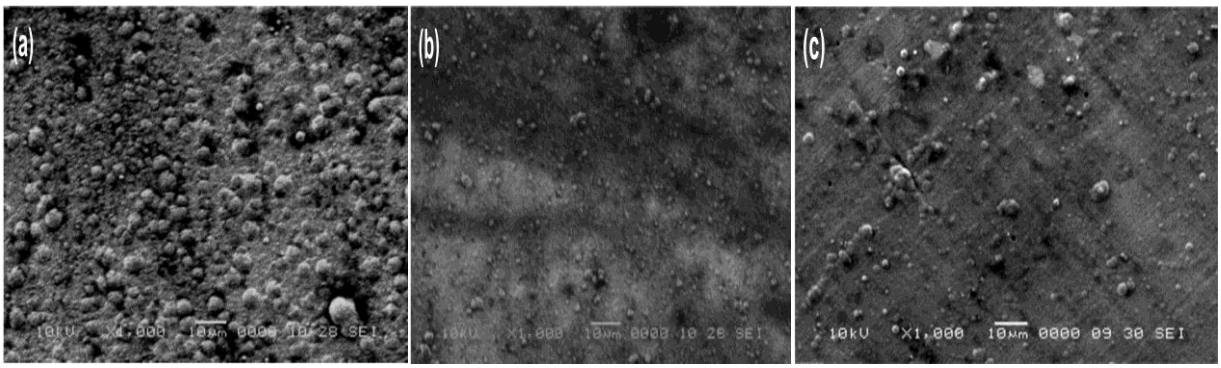

Figure 12. SEM of (a) 82% Ni-18% P alloy; (b) 89% Ni-5.5% P-5.5% Al_2O_3 coating; (c) 90.1% Ni-8% P-1.9% TiO_2 coating.

3.5 Microhardness

The hardness of 86.5% Ni-5% P-Al_2O_3 with 8.5% alumina was observed to be 620 HV_{50}. For Ni-P-TiO_2 with 2% titania, the hardness was 450 HV_{50} without heat treatment. The hardness of Ni-P for a 96 Ni-4 P coating without heat treatment was 490 HV_{50} was increased in the case of the Al_2O_3 addition. The particle percentage in the coatings also affects the hardness value.

3.6 Corrosion behavior

It is clear from the potentiodynamic curves of Fig. 13, and the data in Table 1, that the corrosion current density of the Cu-base (i_{corr} = 6.2359 µA/cm^2) was lowered by coating the copper substrate with Ni-P alloy (i_{corr} = 0.2848 µA/cm^2) with a protection efficiency of more than 95% indicating that, the Ni-P deposits had positive effects on reducing the corrosion rate in the active corrosion region. Generally, nickel electroless plating improve the corrosion resistance due to formation of protective layer of metallic nickel and nickel phosphide that act as barrier to oxygen diffusion to the metal surface.

The incorporation of Al_2O_3 or TiO_2 particles in the coating cause further decrease in the corrosion current density to (i_{corr} = 0.2584 µA/cm^2 and i_{corr} = 0.1723 µA/cm^2), respectively. This implies that the anodic dissolution reaction of the composite coatings was restrained, which effectively decreased the corrosion sensibility of the coated sample in NaCl solution.

The order of corrosion rate is Ni-P-TiO_2 < Ni-P-Al_2O_3 < Ni-P < Cu-base, with a protection efficiency of 97.42, 95.86 and 95.43 %, respectively.

Table 1. Corrosion data, of the Cu-base, Ni-P, Ni-P-Al_2O_3 and Ni-P-TiO_2 in 3.5% NaCl solutions.

	E_{corr} (i=0), mV	I_{corr}, µA/cm^2	Rp kΩ·cm^2	Beta *a*, mV/decade	Beta *c*, mV/decade	Corrosion µm/yr
Cu-base	-315.0	6.2359	1.93	73.40	-82.7	72.40
Ni-P	-225.0	0.2848	57.64	72.74	-89.7	3.30
Ni-P-Al_2O_3	-233.7	0.2584	32.32	56.52	-64.1	3.00
Ni-P-TiO_2	-323.9	0.1723	0.32	57.30	-71.6	2.02

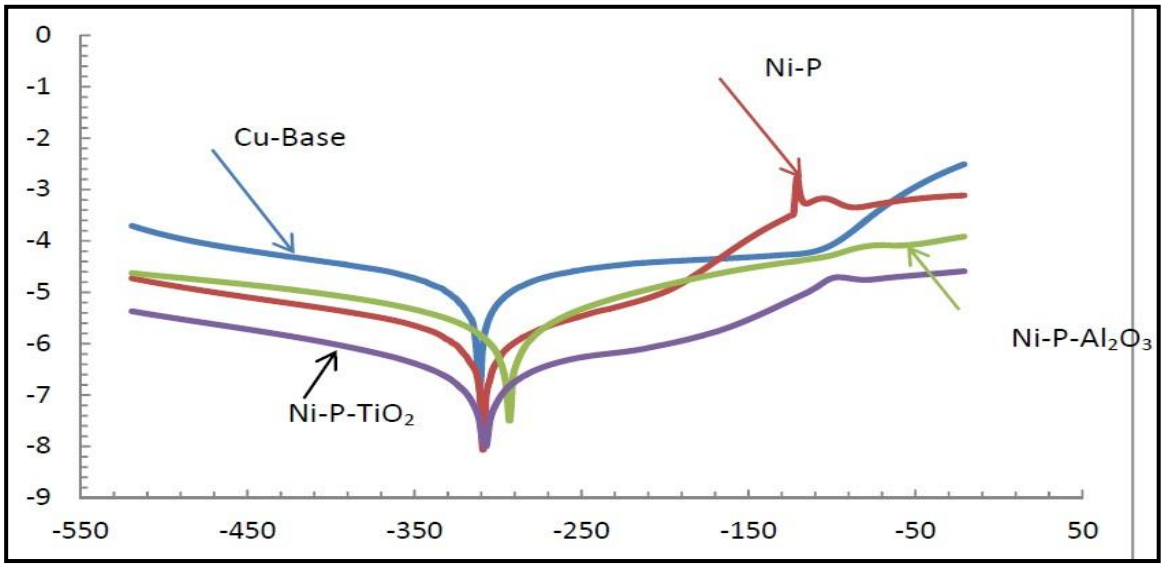

Figure 13. Corrosion behavior, of the Cu-base, Ni-P, Ni-P-Al_2O_3 and Ni-P-TiO_2 in 3.5% NaCl solutions.

4. CONCLUSION

Electroless deposition of Ni-P-Al2O3 and Ni-P-TiO2 in the presence of gluconate as a complexing agent shows that the percentage of incorporated particles in the coating increased with increasing the concentration of particles in the bath. The incorporated alumina and titania particles changed the structure of the Ni-matrix and enhanced the hardness and the corrosion resistance of the coated substrates.

Refereneces

1. Q. Zhao,Y. Liu, H. Müller-Steinhagen, and G. Liu, *Surface and Coatings Technology* 155, (2–3), (2002) 279–284.
2. Pramana *J. Phys*., 65, (5), (2005) 959 -965.
3. U. Erb, *Nanostructured Materials*, 6, (5–8), (1995) 533–538.
4. Robert L. Zeller and Uziel Landau, *J. Electrochem. Soc.* 139 (12), (1992) *3464-3469*.
5. Kang-Heon Hur, Jae-Han Jeong and Dong Nyung Lee, *J. Mater. Sci.*, 25, (5), (1990) 2573-2584.

6. Bernhard Elsener, Maura Crobu, Mariano Andrea Scorciapino and Antonella Rossi, *Journal of Applied Electrochemistry*, 38, (7), (2008) 1053-1060.
7. R. Narayan & B.H Narayan, *J. Electrochem. Soc*., 128 (8), (1981) 1704.
8. A.I. Berner, O.P. Sideleva & V.E. Shub, *J. Analytical Atomic Spectrum*, 5 (4), (1990) 167R.
9. Y.J.M. Park and K.S. Goon, *Han'guk Pyomyon Kinghak Hoechi*, 24, (1991) 222.
10. O. Berkh, S. Eskin, A. Brener & J. Zahavi, *Plating & Surface Finishing*, 82 (1), (1995) 54.
11. K.G. Keong, W. Sha and S. Malinov, *J. Alloys and Compounds*, 334 (1-2), (2002) 192.
12. G. Jiaqiang, *et al.*, *Materials Letters*, 59 (2-3), (2005) 391.
13. J.N. Balaraju, C. Anandan & K.S. Rajam, *Surf. Coat. Technol.*, 200 (12-13), (2006) 3675.
14. A.S. Hamdy, *et al.*, *J. Appl. Electrochem.*, 38 (3), (2008) 385.
15. Y. de Hazan, *et al.*, *J. Colloid & Interface Sci.*, 328 (1), (2008) 103.
16. E.A. Abd El Meguid, S.S. Abd El Rehim and E.M. Moustafa, *Trans. Inst. Met. Fin.*, 77, (1999) 188.
17. S .S. Abd El Rehim, S.M. Sayyah & M.M. El Deeb, *Appl. Surf. Sci.*, 165 (4), (2000) 249 .
18. S.S. Abd El Rehim, S.M. Sayyah, M.M. El Deeb, *Plating & Surface Finishing*, 87 (9), (2000) 93.
19. S.M. Rashwan, A.E. Mohamed, S.M. Abdel Wahaab and M.M. Kamel, *Mansoura Sci. Bull. A: Chem.*, 27, (2000) 121.
20. G.O. Mallory and J.B. Hajdu, *Electroless Plating: Fundamentals and Applications*, NASF, Washington, DC, (1990) p. 386.
21. H. Larhzil, M. Cissé, R. Touir, M. Ebn Touhami and M. Cherkao *Electrochimica Acta*, 53, (2, 1), (2007), Pages 622-628.
22. C. Gabrielli and F. Raulin, *J. Appl. Electrochem*., 1 (3), (1971) 167.
23. Gao Rongjie and Wang Zhichang, *Journal of Inorganic Materials*, 12(4), (1997) 599-603.
24. F. Wünsche, A. Bund and W. Plieth, *J. Solid State Electrochem.* 8 (3), (2004) 209.
25. A. Bund and D. Thiemig, *J. Appl. Electrochem*., 37 (3), (2007) 345.
26. A. Bund & D. Thiemig, *Surf. Coat. Technol*. 201 (2007) 7092.
27. I. Garcia, J. Fransaer and J.P. Celis, *Surf. Coat. Technol.*, 148 (2-3), (2001) 171.
28. T. Lampke, *et al.*, *App. Surf. Sci*., 253 (5), (2006) 2399
29. G. Vidrich, J-F. Castagnet and H. Ferkel, *J. Electrochem. Soc*., 152 (5), (2005) C294.
30. Y. Zhou, H. Zhang and B. Qian, *Appl. Surf. Sci.*, 253 (20), (2007) 8335.